

Polypyrrole–ZnO nanohybrids: effect of CSA doping on structure, morphology and optoelectronic properties

M. A. Chougule · G. D. Khuspe · Shashwati Sen · V. B. Patil

Received: 9 May 2012 / Accepted: 17 July 2012 / Published online: 3 August 2012
© The Author(s) 2012. This article is published with open access at Springerlink.com

Abstract Polypyrrole–ZnO (PPy–ZnO) nanohybrid was prepared from PPy and ZnO nanoparticles (NPs). Nanohybrids of PPy–ZnO were doped with camphor sulfonic acid (CSA) with different weight ratios (10–50 %). The CSA-doped nanohybrids obtained were characterized by X-ray diffraction, FTIR, field emission SEM, UV–vis spectroscopy and electrical transport method. Structural investigations using X-ray diffraction shows new peaks appeared at 15.44° and 17.61° in the XRD pattern of CSA-doped PPy–ZnO nanohybrids belong to CSA. The FTIR spectra confirmed the strong interaction between the CSA and PPy–ZnO nanohybrids. The UV–visible spectrums revealed the enhancement of doping level for the 30 % CSA-doped PPy–ZnO nanohybrid film which is assigned to the existence of greater number of charges on the polymer backbone. The room temperature dc electrical conductivity of CSA-doped PPy–ZnO nanohybrids were observed to depend on the CSA doping and the morphology.

Keywords PPy–ZnO nanohybrid · Structural properties · Optical properties · Electrical properties

Introduction

In recent years, intrinsic conducting polymers with conjugated double bonds have been attracted much attention as

advanced materials. Among those conducting polymers, polypyrrole (PPy) is especially promising for commercial applications because of its good environmental stability, facile synthesis, and higher conductivity than many other conducting polymers. PPy can often be used as biosensors (Vidal et al. 1999; Campbell et al. 1999), gas sensors (Kincal et al. 1998; Kemp et al. 1999), wires (Jerome et al. 1999), microactuators (Smela 1999), antielectrostatic coatings (Ouyang and Li 1997), solid electrolytic capacitor (Arora et al. 2006; Ouyang and Li 1997), electrochromic windows and displays, and packaging, polymeric batteries, electronic devices and functional membranes, etc. (Skotheim 1986; Skotheim et al. 1998; Wallace et al. 1997). PPy coatings have an excellent thermal stability and are good candidate for use in carbon composites (Iroh and Williams 1999). Furthermore, the electrochemical process parameters affecting the properties of the PPy coatings are also investigated (Su and Iroh 1998). PPy can be easily prepared by either an oxidatively chemical or electrochemical polymerization of pyrrole. However, synthetically conductive PPy is insoluble and infusible, which restricts it is processing and applications in other fields.

Shen and Wan (1998) studied the solubility in *m*-cresol, room temperature conductivity, morphology and thermal stability of PPy synthesized by in situ doping polymerization in the present of sulfonic acid. It was noted that good solvating ability of sulfonic acid, such as DBSA and BNSA (5-butyl naphthalene), renders PPy soluble, while sulfonic acids only having large molecular size, such as CSA (camphor sulfonic acid) and MBSA (*p*-methylbenzenesulfonic acid or *p*-toluene sulfonic acid), fail to make PPy soluble. The nature of sulfonic acid also has an influence on morphology of the resulting PPy. The images of PPy doped with CSA, DBSA and MBSA have typical granular morphology, but PPy doped with NSA (*b*-naphthalene) is

M. A. Chougule · G. D. Khuspe · V. B. Patil (✉)
Materials Research Laboratory, School of Physical Sciences,
Solapur University, Solapur 413255, MS, India
e-mail: drvbpatil@gmail.com

S. Sen
Crystal Technology Section, Technical Physics Division, BARC,
Mumbai, India

fibrillar. And it was also observed that PPy doped with NSA and BNSA are thermostable based on the measurement of weight loss. However, it has been found that doping PPy with mixed acid containing CSA and DBSA could get soluble conductive PPy with room temperature conductivity (2–18 S/cm) (Shen and Wan 1998). Pressure effects on the electrical conductivity of doped PPy have been studied (Fedorko 1998). The pressure dependence has characteristics of a phase transition and is interpreted as a conformational wit-rod transition. The pressure effect should be considered in experiments with PPy gas sensors. The pressure and temperature dependences the electric condition of thin films composed of doped PPy microtubules are also measured (Mikat et al. 1999). In addition, it was found that the conductivity of PPy electrochemically polymerized in acrylamide solution is lower than that of PPy prepared in the absence of acrylamide (Sarac et al. 1998). The difference is attributed to the insulating effect of acrylamide. Besides above, synthesis of nanostructures composed of PPy can enhance in electronic conductivity compared to analog polymer bulk conductivity (Duchet et al. 1998).

The syntheses of PPy–ZnO nanoparticles with different combinations of the two materials have attracted more and more attention, since they have interesting physical properties and potential applications. These particles not only combine the advantageous properties of ZnO and PPy, but also exhibit many new characteristics that single-phase materials do not have (Chougule et al. 2010).

In this article, we report the synthesis of CSA-doped PPy–ZnO nanohybrid films by spin coating technique and study of their microstructural, morphological, optical and charge transport properties.

Experimental methods

Preparation of PPy–ZnO nanohybrid

PPy was synthesized by polymerization of pyrrole in the presence of ammonium persulfate as an oxidant by chemical oxidative polymerization method (Chougule et al. 2011). ZnO (NPs) was synthesized by sol–gel method using zinc acetate as a source material (Patil et al. 2011) and such obtained PPy and ZnO (NPs) were mixed together in 50 % weight ratio and grinded in agate mortar for 1 h to get PPy–ZnO (50 %) nanohybrids (Chougule et al. 2011, 2012). In our previous report (Chougule et al. 2011), it was found that the PPy nanohybrids filled with different loadings of ZnO nanoparticles, the particles are closely packed and no bare nanoparticles are observed even at the highest loading of 50 wt %, which suggests the feasibility of this method to fabricate well-dispersed nanoparticles with uniform coating layer.

Preparation of CSA-doped PPy–ZnO nanohybrids

The CSA-doped PPy–ZnO nanohybrids were prepared by adding CSA with different weight ratios (10–50 %) into the PPy–ZnO (50 %) nanohybrid. These CSA-doped nanohybrids were dissolved in m-cresol and stirring it for 11 h at room temperature. Thin films of CSA-doped nanohybrids were prepared on glass substrate by spin coating technique at 3,000 rpm for 40 s and dried on hot plate at 100 °C for 10 min (Chougule et al. 2011, 2012).

Characterization of CSA-doped PPy–ZnO nanohybrid

To determine the structure and properties of the CSA-doped nanohybrids using techniques, such as X-ray diffraction (Model: Philips PW1710 diffractometer (Holland) with CuK_α radiation at step width 0.02°, step time 1.25 s, and $\lambda = 1.5406 \text{ \AA}$), Fourier transform infra red (FTIR) spectroscopy (Model: Perkin Elmer 100 spectrophotometer, Santa Clara, CA, USA), Field emission scanning electron microscopy (FESEM Model: MIRA3 TESCAN, USA operating at 20 kV), UV–vis spectra of the samples (Model: Simandzu-100 UV–Vis spectrophotometer, Kyoto, Japan) were carried out. For conductivity measurement, two electrodes, separated by 10 mm, were deposited on CSA-doped PPy–ZnO film using silver paint. The room temperature dc electrical conductivity CSA doped PPy–ZnO nanohybrids were measured using custom-made two probe techniques. The thicknesses of the films were measured by using an AMBIOS make XP-1 surface profiler with 1 Å vertical resolution (Table 1).

Results and discussion

Structural analysis

The X-ray diffraction spectra of the PPy–ZnO (50 %) and PPy–ZnO–CSA (10–50 wt. %) nanohybrid are as shown in

Table 1 Effect of CSA doping on thin-film properties of PPy–ZnO nanohybrids

CSA doping in PPy–ZnO (%)	Particle size from XRD (nm)	Grain size from FESEM (nm)	Base resistivity (MΩ)	Conductivity (S/cm)
0	39.56	133	7.01	1.42×10^{-7}
10	59.66	120	1.55	6.47×10^{-7}
20	62.65	110	1.33	7.51×10^{-7}
30	62.77	111	1.18	8.49×10^{-7}
40	63.85	166	2.50	3.83×10^{-7}
50	65.94	203	3.44	2.39×10^{-7}

Figs. 1, 2. The patterns exhibit sharp and well-defined peaks, indicating the crystallinity of synthesized materials. XRD patterns of PPy–ZnO–CSA (10–50 wt. %) have shown that all major diffraction peaks of nanocrystalline ZnO with the standard JCPDS values (JCPDS No. 79-0208), which shows wurtzite structure of ZnO and are

in the same peak angle positions (Chougule et al. 2011; Patil et al. 2011). When compared with Fig. 2a, new peaks observed at $2\theta = 15.44$ and 17.61° in the crystal pattern of PPy–ZnO–CSA belong to CSA (Tai et al. 2008) and more significant in the doping patterns appeared in Fig. 2b–f.

Fig. 1 Flow diagram of synthesis and deposition of CSA-doped PPy–ZnO nanohybrids

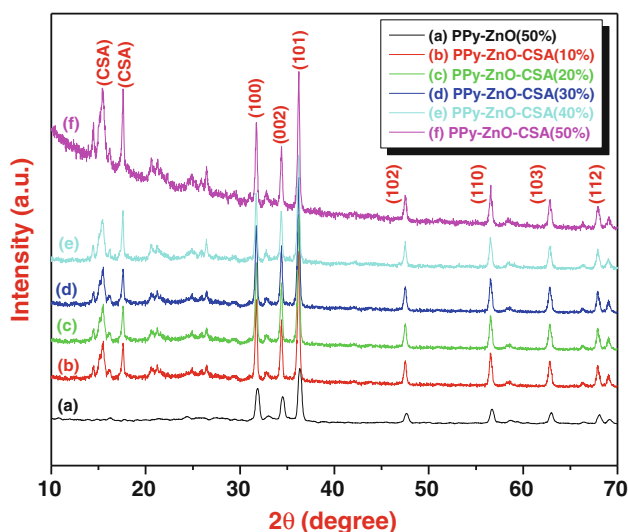
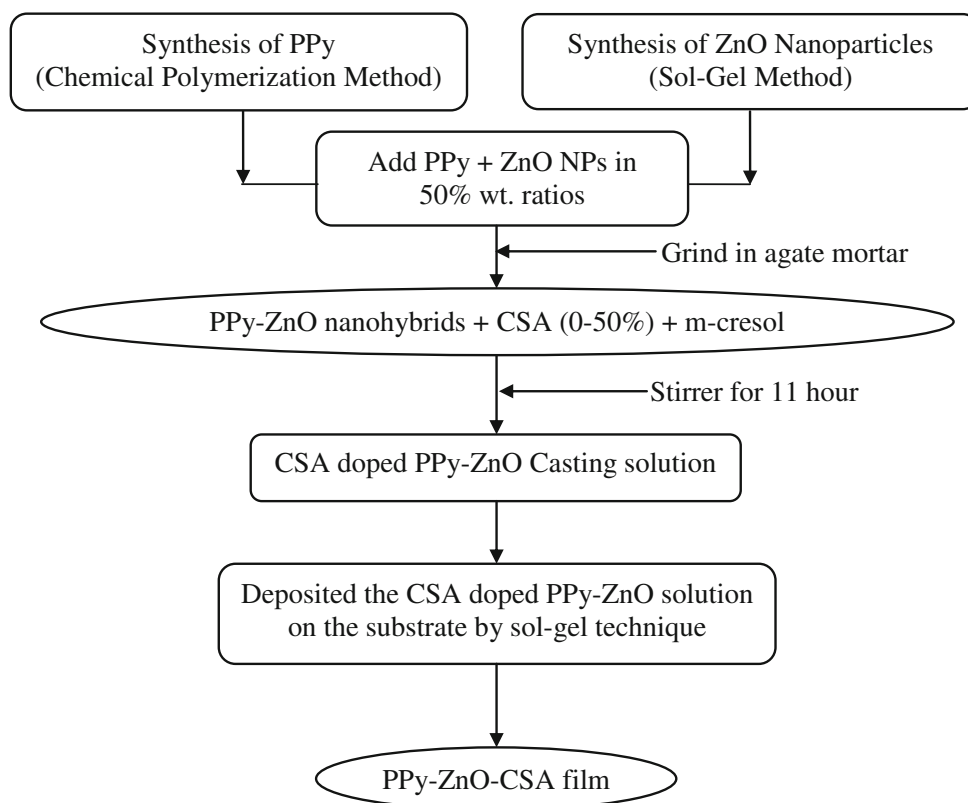


Fig. 2 X-ray diffraction pattern of a PPy–ZnO (50 %), b PPy–ZnO–CSA (10 %), c PPy–ZnO–CSA (20 %), d PPy–ZnO–CSA (30 %), e PPy–ZnO–CSA (40 %), f PPy–ZnO–CSA (50 %)

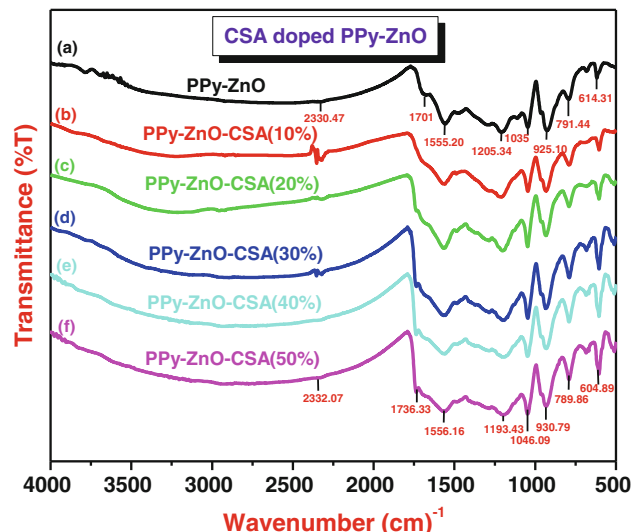


Fig. 3 FTIR spectra of a PPy–ZnO, b PPy–ZnO–CSA (10 %), c PPy–ZnO–CSA (20 %), d PPy–ZnO–CSA (30 %), e PPy–ZnO–CSA (40 %) and f PPy–ZnO–CSA (50 %)

Fourier transform infrared spectroscopy analysis

Figure 3 shows the FTIR spectra of PPy–ZnO and CSA doped with (10–50 %) weight ratios into the PPy–ZnO (50 %) nanohybrids. For PPy–ZnO nanohybrid FTIR spectra (Fig. 3a), all the characteristics absorption peaks of PPy–ZnO nanohybrid are observed, that is, 614 cm^{-1} ($=\text{C}-\text{H}$ wagging), $1,035\text{ cm}^{-1}$ ($=\text{C}-\text{H}$ in-plane vibration), $1,701\text{ cm}^{-1}$ ($\text{C}=\text{N}$ bond) (Chougule et al. 2011). The spectrum for CSA-doped PPy–ZnO nanohybrid (Fig. 3b, f) shows some shift in the wavenumber as compared to PPy–ZnO nanohybrid. The most prominent changes are (1) a shift of $=\text{C}-\text{H}$ in-plane vibration peak to high value,

i.e. from $1,035$ to $1,046\text{ cm}^{-1}$, (2) a shift of $\text{C}=\text{N}$ bond peak to high value, i.e. from $1,701$ to $1,736\text{ cm}^{-1}$, (3) a shift of $=\text{C}-\text{H}$ wagging to a lower value i.e. from 614 to 604 cm^{-1} . Because the frequency of a vibration is directly proportional to the strength of the bond (i.e. force constant), a shift in $=\text{C}-\text{H}$ in-plane vibration peak to higher side indicate that the electrons are more localized in the CSA-doped PPy–ZnO nanohybrid. It is also observed that the polymer is protonated in part by surface anions is demonstrated by the presence of the peak at 614.31 cm^{-1} , which is attributed to a stretching vibration in the surface anion (He et al. 2003). The presence of CSA is confirmed by the bonds at $1,046\text{ cm}^{-1}$ (SO_3^{3-})

Fig. 4 FESEM of **a** PPy–ZnO (50 %), **b** PPy–ZnO–CSA (10 %), **c** PPy–ZnO–CSA (20 %), **d** PPy–ZnO–CSA (30 %), **e** PPy–ZnO–CSA (40 %) and **f** PPy–ZnO–CSA (50 %)

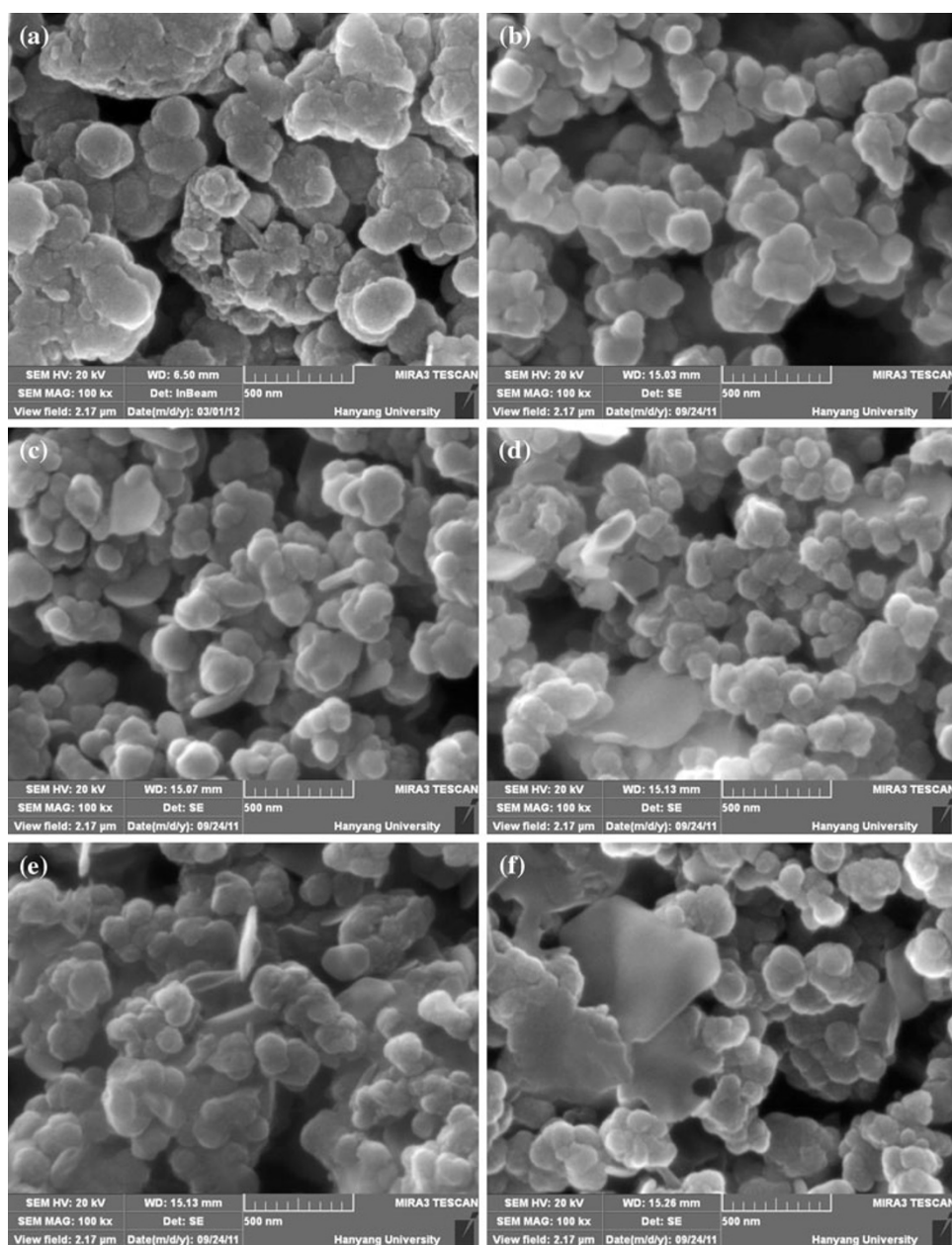
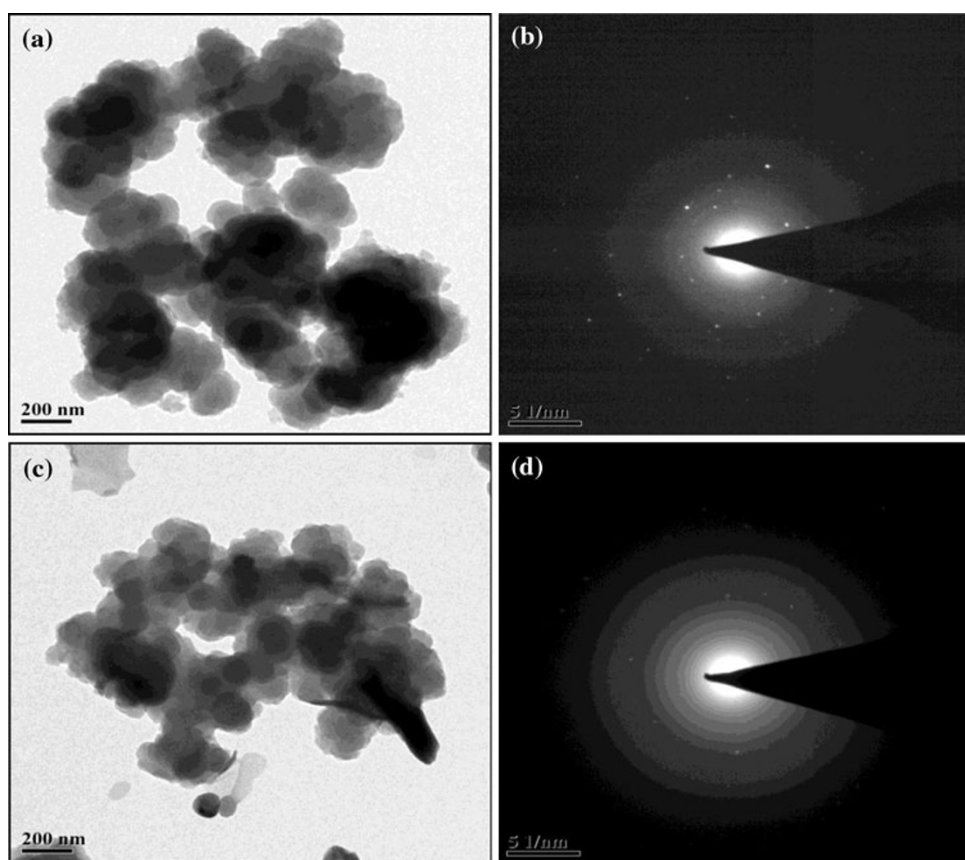


Fig. 5 Transmission electron micrographs of PPy–ZnO (50 %) and PPy–ZnO–CSA (30 %) thin films **a** microstructure of PPy–ZnO (50 %), **b** selected area electron diffraction pattern of PPy–ZnO (50 %), **c** microstructure of PPy–ZnO–CSA (30 %), **d** selected area electron diffraction pattern of PPy–ZnO–CSA (30 %)



(Tai et al. 2008; He et al. 2003; Stejkal et al. 1998; Konyushenko et al. 2006).

Surface morphology analysis

Figure 4 shows the field emission scanning electron micrographs (FESEM) of PPy–ZnO (50 %) and PPy–ZnO–CSA (10–50 %) nanohybrid films at $\times 100,000$ magnification, respectively. Figure 4a shows the microstructure of a PPy–ZnO (50 %) nanohybrid film has a uniform distribution of ZnO NPs into PPy matrix indicates that ZnO NPs interact with PPy (Chougule et al. 2011). The FESEM micrograph of CSA (10–50 wt %) doped with PPy–ZnO (50 %) nanohybrids are shown in Fig. 4b–f. The change in the surface morphology was observed with increasing content of CSA into the PPy–ZnO nanohybrid. At lower content of CSA (≤ 30 %), the uniform granular dense interconnected morphology attributed to the homogeneous dispersion of CSA into the PPy–ZnO nanohybrid. At higher content of CSA (30 %), porous granular morphology accumulates with voids are observed. Similar change in morphology due to addition of CSA into PPy matrix was observed by Wang et al. (2001). It is revealed that 30 % CSA-doped PPy–ZnO nanohybrid shows homogeneous, large area, dense granular morphology suitable for gas sensing application and energy storage devices (Pawar et al. 2011).

Micro structural analysis

Transmission electron micrographs (TEM) image of PPy–ZnO (50 %) nanohybrid is shown in Fig. 5a which reveals the dispersion of ZnO NPs (light shaded) in PPy matrix (dark shaded) with grain size of about ~ 100 –200 nm. The ZnO NPs are coated with PPy and embedded in the bulk PPy matrix with a small fraction of the coated particles adhered to the matrix surface (Fig. 5a). The well-dispersed PPy–ZnO nanohybrids with a diameter of ~ 92 nm are fully wrapped with a thin layer of surfactant CSA is shown in Fig. 5c. Figure 5b and d shows selected area electron diffraction (SAED) pattern of PPy–ZnO (50 %) and PPy–ZnO–CSA (30 %) thin films, respectively. The different arrangement of dominant diffracted rings indicates a phase evolution of crystalline grains.

Electrical conductivity analysis

Figure 6 shows the variation of electrical conductivity ($\log \sigma$) with increasing doping concentration of CSA into PPy–ZnO nanohybrid measured using custom fabricated two probe method at room temperature. It is observed that the room temperature conductivity of PPy–ZnO nanohybrid increases from 1.42×10^{-7} to 8.48×10^{-7} S/cm as doping concentration of CSA increased from 0 to 30 %. This may be

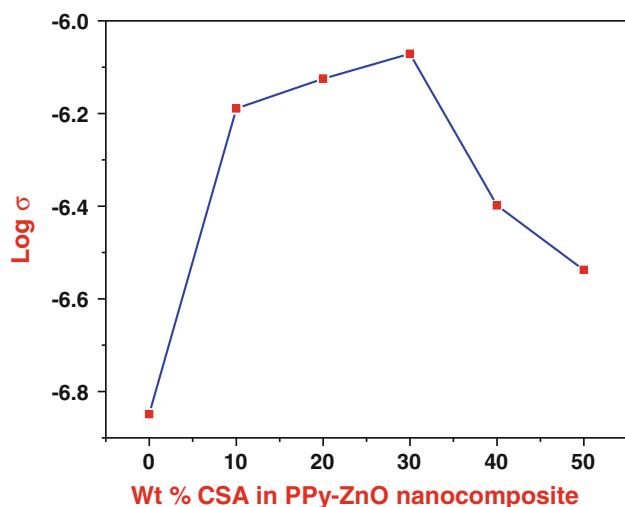


Fig. 6 Variation of $\log \sigma$ versus the content of CSA in PPy-ZnO nanohybrids

attributed to the doping of CSA which maximizes the number of carriers. The highest number of carriers can be connected with the delocalization effect of doping process and formation of the polarons or bipolarons in the composite structure, thus enhancing the conductivity of composite (Pawar et al. 2011; Maminya et al. 2002; Huang 2002). At higher (≥ 30 %) content of CSA, the conductivity goes on decreasing (3.83×10^{-7} to 2.39×10^{-7} S/cm). This decrease in conductivity may be due to the accumulation of charge carrier. This is also confirmed from FESEM observation.

Optical studies

Band gap analysis

Figure 7 shows a plot of $(\alpha h\nu)^2$ versus photon energy ($h\nu$) for different weight ratios of CSA-doped PPy-ZnO nanohybrid deposited onto glass substrates. The optical absorption data were analyzed using the following classical relation (Raut and Chougule 2012)

$$\alpha = \alpha_0(h\nu - E_g)^n/h\nu$$

where ' α_0 ' is a constant, ' E_g ' the semiconductor band gap and ' n ' a number equal to 1/2 for direct gap and 2 for indirect gap compound.

The values of the optical band gap decreases slightly (3.89–3.71 eV) as doping concentration of CSA increased from 10 to 30 %. The decrease in band gap indicates to improve the conductivity of the film due to the effect of CSA surfactant into the PPy-ZnO nanohybrids. It was also observed that the optical band gap increases (3.75–3.79 eV) as doping concentration of CSA increased from 40 to 50 %. This is increased band gap correlated with decrease in conductivity of 40–50 % CSA doped in PPy-ZnO nanohybrids.

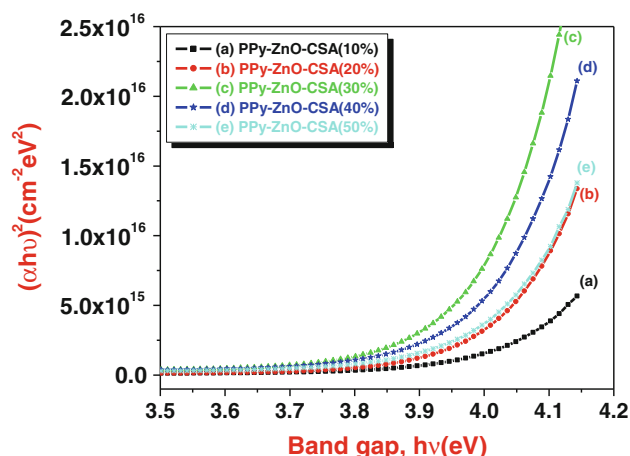


Fig. 7 Plot of $(\alpha h\nu)^2$ versus $(h\nu)$ for different CSA doping in PPy-ZnO nanohybrids

Conclusion

The CSA-doped PPy-ZnO nanohybrid films were successfully prepared by spin coating technique on glass substrates. The doping effect of CSA on structural, morphological, electrical and optical properties of PPy-ZnO nanohybrids were investigated by XRD, FTIR, FESEM, UV-visible and two probe techniques. The morphological studies (FESEM) show uniform granular porous morphology of 30 % CSA-doped PPy-ZnO nanohybrid. From FTIR spectra, it is revealed that the characteristic absorption peaks of PPy-ZnO nanohybrids shifted by significant amount into CSA-doped PPy-ZnO nanohybrid, which indicates that the different interfacial interactions between the CSA and PPy-ZnO nanohybrid. The UV spectra shows the band gap of PPy-ZnO nanohybrid decreases with increasing CSA doping confirmed the interaction between CSA and PPy-ZnO nanohybrids. The dc electrical conductivity increases with increasing CSA into PPy-ZnO nanohybrids up to 30 % and then decreases due to the accumulation of charge carrier.

Acknowledgments The authors (VBP) are grateful to DAE-BRNS, for financial support through the scheme no. 2010/37P/45/BRNS/1442.

Open Access This article is distributed under the terms of the Creative Commons Attribution License which permits any use, distribution, and reproduction in any medium, provided the original author(s) and the source are credited.

References

- Arora K, Chaubey A, Singhal R, Singh RP, Pandey MK, Samanta SB, Malhotra BD, Chand S (2006) Application of electrochemically prepared polypyrrole-polyvinyl sulphonate films to DNA biosensor. *Bio-sen Bioelectr* 21(9):1777–1783

- Campbell TE, Hodgson AJ, Wallace GG (1999) Incorporation of erythrocytes into polypyrrole to form the basis of a biosensor to screen for rhesus (d) blood groups and rhesus (d) antibodies. *Electroanalysis* 11(4):215
- Chougule MA, Pawar SG, Godse PR, Mulik RN, Sen S, Patil VB (2011) Synthesis and characterization of polypyrrole (PPy) thin films. *Soft Nanosci Lett* 1:6–10
- Chougule MA, Sen S, Patil VB (2012) Facile and efficient route for preparation of polypyrrole–ZnO nanocomposites: microstructural, optical and charge transport properties. *J Appl Polym Sci*. doi:10.1002/app.36475
- Chougule MA, Dalvi DS, Mali S, Patil PS, Moholkar AV, Agawane GL, Kim JH, Sen S, Patil VB (2012b) Novel method for fabrication of room temperature polypyrrole–ZnO nanocomposite NO₂ sensor. *Measurement* 45:1989–1996
- Duchet J, Legras R, Sophic SC (1998) Chemical synthesis of polypyrrole: structure–properties relationship. *Synth Met* 98:113
- Fedorko P, Skákalová V (1998) Low pressure effect in the electrical conductivity of doped polypyrrole. *Synth Met* 94:279
- He C, Tan Y, Li Y (2003) Conducting polyaniline nanofiber networks prepared by the doping induction of camphor sulfonic acid. *J Appl Polym Sci* 87(9):1537–1540
- Huang JC (2002) Carbon black filled conducting polymers and polymer blends. *Adv Polym Technol* 21(4):299–313
- Iroh JO, Williams C (1999) Formation of thermally stable polypyrrole–naphthalene/benzene sulfonate-carbon fiber composites by an electrochemical process. *Synth Met* 99(1):1–8
- Jerome C, Labaye D, Bodart I, Jerome R (1999) Electrosynthesis of polyacrylic/polypyrrole composites: formation of polypyrrole wires. *Synth Met* 101:3
- Kemp NT, Flanagan GU, Kaiser AB, Trodahl HJ, Chapman B, Partridge AC, Buckley RG (1999) Temperature-dependent conductivity of conducting polymers exposed to gases. *Synth Met* 101(2):434–435
- Kincal D, Kamer A, Child AD, Reynold JR (1998) Conductivity switching in polypyrrole-coated textile fabrics as gas sensors. *Synth Met* 92:53
- Konyushenko E, Stejkal J, Trchova M, Hradil J, Kovarova J, Prokes J, Cieslar M, Hwang JY, Chen KH, Sapurina I (2006) Multi-wall carbon nanotubes coated with polyaniline. *Polymer* 47:5715–5723
- Maminya YP, Davydenko VV, Pissis P, Lebedev EV (2002) Electrical and thermal conductivity of polymers filled with metal powders. *Eur Polym J* 38:1887
- Mikat J, Orgzall I, Lorenz B, Sapp S, Martin CR, Jennifer JL, Hochheimer HD (1999) High-pressure low-temperature electrical properties of template-synthesized polypyrrole at low synthesis temperature: dimensional crossover under pressure. *Phys B* 265(1–4):154
- Ouyang JY, Li YF (1997) Great improvement of polypyrrole films prepared electrochemically from aqueous solutions by adding nonaphenol polyethyleneoxy (10) ether. *Polymer* 38:3997–3999
- Patil SL, Chougule MA, Pawar SG, Raut BT, Sen S, Patil VB (2011) New process for synthesis of ZnO thin films: microstructural, optical and electrical characterization. *J Alloy Compd* 509:10055–10061
- Pawar SG, Patil SL, Chougule MA, Raut BT, Godase PR, Mulik RN, Sen S, Patil VB (2011a) New method for fabrication of CSA doped PANi–TiO₂ thin-film ammonia sensor. *IEEE Sensor J* 11(11):2980–2985
- Pawar SG, Patil SL, Chougule MA, Raut BT, Patil VB (2011b) Camphor sulfonic acid doped polyaniline–titanium dioxide nanocomposite: synthesis, structural, morphological, and electrical properties. *Int J Polym Mater* 60:979–987
- Raut BT, Chougule MA, Sen S, Pawar RC, Lee CS, Patil VB (2012) Novel method of fabrication of polyaniline–CdS nanocomposites: structural, morphological and optoelectronic properties. *Ceram Int* 38:3999–4007
- Sarac AS, Sonmez G, Ustamehinoglu B (1998) Electrochemical polymerization of pyrrole in acrylamide solution. *Synth Met* 98:177
- Shen YQ, Wan MX (1998a) In situ doping polymerization of pyrrole with sulfonic acid as a dopant. *Synth Met* 96(2):127–132
- Shen YQ, Wan MX (1998b) Soluble conducting polypyrrole doped with DBSA–CSA mixed acid. *J Appl Polym Sci* 68(8):1277–1284
- Skotheim TA (ed) (1986) Handbook of conducting polymers, vols I and II, Marcel Dekker, New York
- Skotheim TA, Elsenbaumer R, Reynolds J (eds) (1998) Handbook of conducting polymers. Marcel Dekker, New York
- Smela E (1999) Microfabrication of PPy microactuators and other conjugated polymer devices. *J Micromech Microeng* 9(1):1–18
- Stejkal J, Spurina I, Trchova M, Prokes J, Krivka J, Tobolkova E (1998) Solid state protonation and electrical conductivity of polyaniline. *Macromolecules* 31:2218–2222
- Su W, Iroh JO (1998) Effects of electrochemical process parameters on the synthesis and properties of polypyrrole coatings on steel. *Synth Met* 95:159
- Tai H, Juang Y, Xie G, Yu J, Chen X, Ying Z (2008) Influence of polymerization temperature on NH₃ response of PANI/TiO₂ thin film gas sensor. *Sens Actuat B* 129:319–326
- Vidal JC, Garcia E, Castillo JR (1999) In situ preparation of a cholesterol biosensor: entrapment of cholesterol oxidase in an over oxidized polypyrrole film electrodeposited in a flow system: determination of total cholesterol in serum. *Anal Chim Acta* 385(1–3):213–222
- Wallace GG, Spinks G, Teasdale PR (1997) Conductive electroactive polymers. Technomic, New York
- Wang L-X, Li X-G, Yang Y-L (2001) Preparation, properties and applications of polypyrroles. *React Funct Polym* 47:125–139